ACS Medicinal Chemistry Letters

Letter

pubs.acs.org/acsmedchemlett

Fragment-Based Discovery of 6-Azaindazoles As Inhibitors of Bacterial DNA Ligase

Steven Howard,*[,†] Nader Amin,[†] Andrew B. Benowitz,[‡] Elisabetta Chiarparin,[†] Haifeng Cui,*[,‡] Xiaodong Deng,[‡] Tom D. Heightman,[†] David J. Holmes,[‡] Anna Hopkins,[†] Jianzhong Huang,[‡] Qi Jin,[‡] Constantine Kreatsoulas,[‡] Agnes C. L. Martin,[†] Frances Massey,[†] Lynn McCloskey,[‡] Paul N. Mortenson,[†] Puja Pathuri,[†] Dominic Tisi,[†] and Pamela A. Williams[†]

[†]Astex Pharmaceuticals Inc., 436 Cambridge Science Park, Milton Road, Cambridge CB4 0QA, United Kingdom

[‡]GlaxoSmithKline, Infectious Diseases TAU, 1250 South Collegeville Road, Collegeville, Pennsylvania 19426, United States

Supporting Information

ABSTRACT: Herein we describe the application of fragment-based drug design to bacterial DNA ligase. X-ray crystallography was used to guide structure-based optimization of a fragment-screening hit to give novel, nanomolar, AMP-competitive inhibitors. The lead compound **13** showed antibacterial activity across a range of pathogens. Data to demonstrate mode of action was provided using a strain of *S. aureus*, engineered to overexpress DNA ligase.

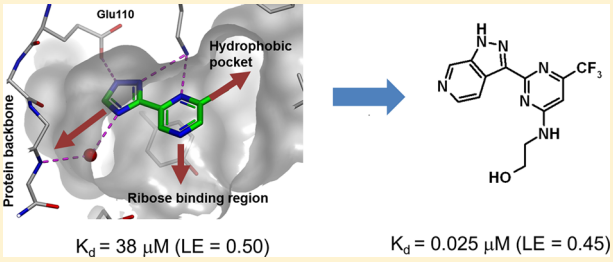

KEYWORDS: *Bacterial DNA ligase, S. aureus, fragment-based drug design, structure-based optimization*

Bacterial DNA ligase (LigA) is an NAD^+-dependent enzyme, which is essential for DNA replication and has attracted interest as a novel target for antibacterial therapy.[1] LigA is responsible for ligating two strands of DNA via the formation of a phosphodiester bond between the 3′-hydroxyl end of one oligonucleotide and the 5′-phosphate end of another.[2,3] This process involves a three-step mechanism. Initially, reaction between NAD^+ and an active-site lysine leads to an adenylated form of the protein. Enzyme-bound AMP is then transferred to the 5′-phosphate end of a nicked DNA strand. Finally, attack on the AMP-DNA bond by the 3′-hydroxyl of a second strand of DNA seals the phosphate backbone and releases AMP. LigA has been shown to be essential for viability in all Gram-positive and Gram-negative organisms tested to date.[4,5] It is highly conserved across bacterial species and is phylogenetically quite distinct from its human, ATP-dependent, counterpart. This provides encouragement that inhibitors of LigA may exhibit both broad-spectrum antibacterial activity and selectivity over human isozymes.[6]

Widespread bacterial resistance to current classes of approved antibiotics has led to an unmet medical need for compounds with novel modes of action that are not compromised by pre-existing resistance mechanisms.[7] As a clinically unexploited target, inhibitors of LigA would fall into this category, and several classes of compounds have been reported in the literature.[8−11] In most cases, high throughput screening (HTS) hits have provided chemical starting points, which were then optimized, often using structure-based drug design. Notable examples, shown to exhibit target-mediated antibacterial activity, include the adenosine analogue **1** and naphthyridine **2** (Figure 1).[8,10]

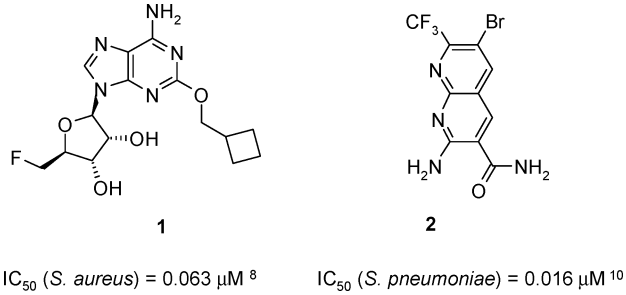

Figure 1. Inhibitors of DNA ligase described in the literature.[8,10]

Although in cases such as LigA molecular targeted HTS has delivered chemical leads, success rates from antibacterial HTS are typically lower than for targets from other therapeutic areas.[12] In this letter, we describe an alternative approach to the discovery of LigA inhibitors using fragment-based drug design (FBDD).[13] FBDD has become established as an approach for the generation of chemical leads for drug targets and has been employed in a variety of therapeutic areas, including antibacterials.[14,15] In this approach specialized detection methods are used to identify small chemical compounds,

Received: August 22, 2013
Accepted: October 10, 2013
Published: October 18, 2013

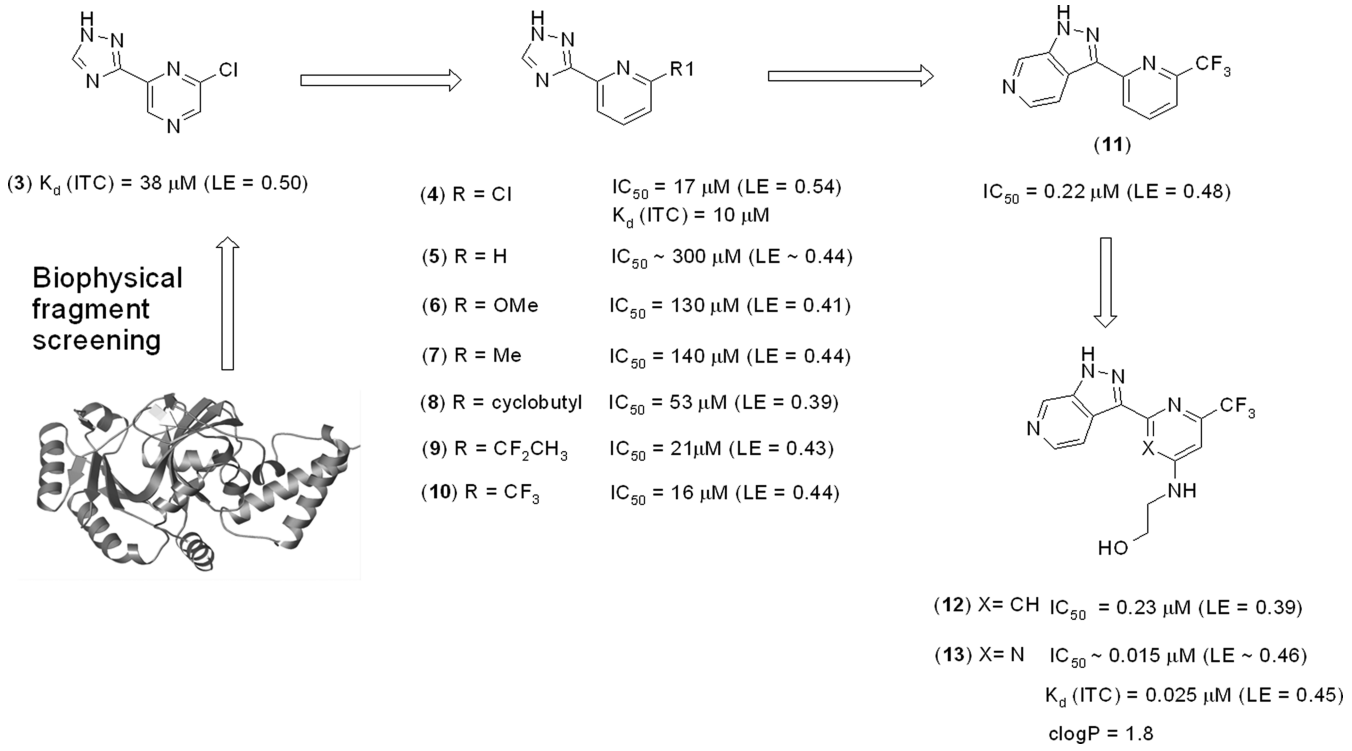

Figure 2. Fragment optimization and growth of **3** toward **13**. Data presented as K_d (ITC) or IC_{50} (biochemical assay) using DNA ligase from *S. aureus*.

fragments (MW ≤ 16 heavy atoms) that bind to the drug target, and structural biology is usually employed to establish their binding mode and to facilitate their optimization. A key feature of fragment-derived leads is that they are, on average, significantly smaller and less lipophilic than historical leads derived from HTS.[16] Given that successful antibiotics are typically associated with lower lipophilicity than other drug classes,[17,18] FBDD seems well suited to this therapeutic area. To our knowledge, this is the first published example of a fragment-derived LigA inhibitor.

An essential prerequisite to a successful fragment screening cascade for LigA was the identification of a stable, deadenylated, soakable crystal form of the protein. Constructs from multiple pathogens, including *E. faecalis*, *H. influenzae*, *S. aureus*, and *E. coli*, were prepared and subject to deadenylation by incubation with nicotinamide mononucleotide (NMN). LigA constructs showing reproducible and sustained levels of complete deadenylation (as determined by mass spectrometry) were progressesd to large scale crystallization trials. Of these, LigA from *S. aureus* provided the most stable soakable crystal form of the enzyme, and this was selected as the preferred system for X-ray crystallographic screening. Approximately 1500 compounds from our fragment library were then screened using a combination of high throughput LigA X-ray crystallography, ligand observed NMR (via water LOGSY), and a thermal shift (T_m) assay. Hits were then followed up using isothermal titration calorimetry (ITC) to determine binding affinities and ligand efficiencies (LE).[19]

The starting point for chemical optimization was provided by the fragment-based screening hit **3** [Figure 2, K_d (ITC) = 38 μM, ligand efficiency, LE = 0.50]. The X-ray crystallographic structure of LigA (*S. aureus*) in complex with **3** revealed that the fragment binds in the AMP pocket and forms hydrogen bonds with the side chains of Lys283 and Glu110 (Figure 3a). An additional, water-mediated, hydrogen bond exists between the triazole nitrogen and the protein backbone NH of Ile113. Further interaction is provided by the side chain of Tyr219, which partially stacks with the pyrazine ring.

Pyrazine **3** offered an attractive starting point for structure-based optimization for three reasons. First, **3** was one of the most ligand efficient hits observed for LigA. Second, the 2-chloro group partly fills the hydrophobic pocket (Figure 3a), a region of the active site which is occluded in the human form of the enzyme, providing an opportunity to obtain selectivity.[20] Third, replacing the pyrazine with a pyridine would provide a growth vector to explore the ribose-binding region, via the pyridyl 4-position, provided this replacement was tolerated.

The pyridine analogue **4** [K_d (ITC) = 10 μM, IC_{50} = 17 μM, LE = 0.54] (Figure 2) was prepared, which, gratifyingly, showed improved activity over the fragment hit **3**. One concern was the potentially reactive chlorine at position 2. To mitigate this risk, a number of alternative groups were explored at this position. Deletion of the 2-substituent (compound **5**) or introduction of an electron donating substituent (e.g., OMe analogue **6**) were both detrimental to activity. 2-Alkyl substituents (e.g., cyclobutyl **8**), although appearing to fill the hydrophobic region more effectively than chlorine, surprisingly offered little advantage. These findings suggested that the electronics of the 2-substituent may be more important than sterics and that increasing the electron withdrawing nature of the alkyl group could be advantageous. The trifluoromethyl analogue **10** (IC_{50} = 16 μM, LE = 0.44) was synthesized, which proved equipotent with **4**, albeit with a modest loss in ligand efficiency.

As described above, one of the interactions formed by these compounds is a water-mediated hydrogen bond between the triazole 4-position nitrogen and the backbone NH of Ile 113 (shown in Figure 3a). Our next strategy was to expand the

dx.doi.org/10.1021/ml4003277 | *ACS Med. Chem. Lett.* 2013, 4, 1208−1212

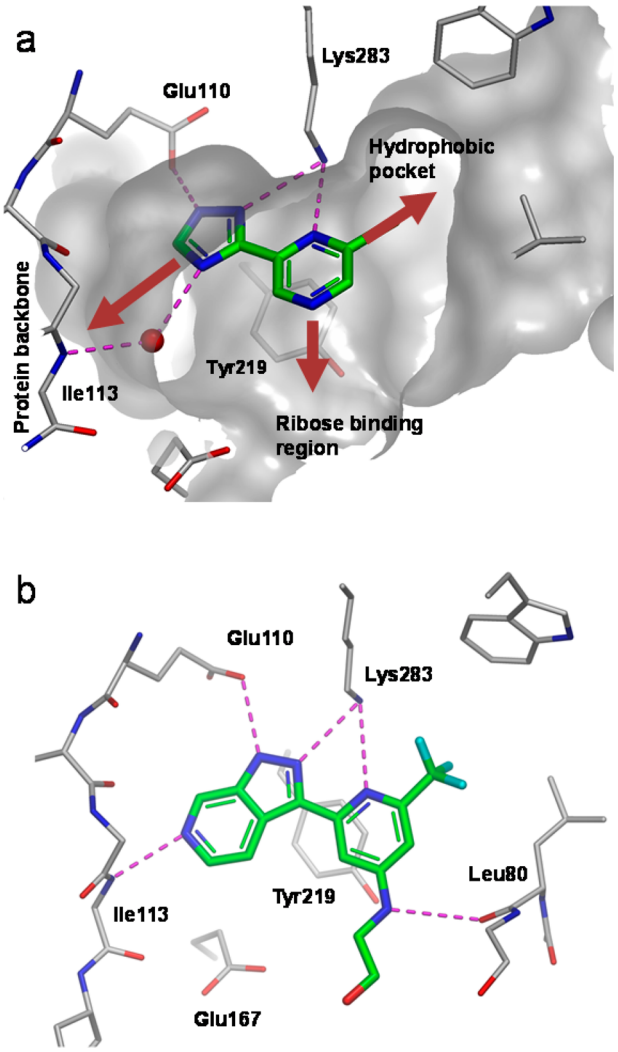

Figure 3. (a) X-ray crystal structure of fragment **3** bound to LigA (*S. aureus*) showing key hydrogen bonds (purple dotted lines), a key water molecule (red sphere), and partially resected Connoly surface. (gray). Growth vectors toward the hydrophobic pocket, ribose binding region, and the protein backbone are shown by the red arrows. (b) X-ray crystal structure of **12** bound to LigA (*S. aureus*).

triazole ring, in order to fill the pocket more effectively, displace this bridging water molecule and form a direct hydrogen bond with Ile 113.

To this end, the 6-azaindazole analogue **11** (IC_{50} = 0.22 μM, LE = 0.48) was prepared, which proved to be ~70-fold more potent than **10**. An X-ray structure of **11** could not be obtained, which we ascribed to the low solubility (solubility = 12 μg/mL)[21] of this compound. Next, attention was turned toward exploring substitution at the pyridine 4-position in order to access the ribose-binding pocket. The more soluble ethanolamine derivative **12** (solubility = 113 μg/mL) was prepared, which was comparable in potency to **11** and enabled an X-ray structure of the protein−ligand complex to be obtained. The structure of **12** complexed with DNA ligase clearly shows N6 of the 6-azaindazole making the intended hydrogen-bond to the backbone NH of Ile113 (Figure 3b). The other interactions are conserved. An inspection of the ribose-binding region indicates a hydrogen-bond between the backbone carbonyl of Leu80 and the 4-aminopyridine substituent. However, the electron density around the last two atoms of the ethanolamine chain was ambiguous, and therefore, the exact position of the OH group is uncertain. Although the ethanolamine motif did not improve potency in the biochemical assay, it did result in **12** being the first analogue to show signs of antibacterial activity, particularly against *S. aureus* [MIC *S.aureus* (Oxford) = 8 μg/mL] (Table 1).

Table 1. MIC Data for Compounds 1, 12, and 13

	MIC (μg/mL)		
compd	1[a]	12	13
Gram-Positive Pathogens			
S. aureus Oxford	8	8	4
S. pneumoniae 1629	2	64	2
S. pyogenes 1307006P	8	128	8
Gram-Negative Pathogens			
H. influenzae H128	16	128	16
E. coli 7623	>128	>128	>128
K. pneumonia 1161486	>128	>128	>128
P. aeruginosa PAO(MV)	>128	>128	>128
A. baumannii BM4454	>128	>128	>128
Gram-Negative Efflux Knockout Strains[b]			
H. Influenzae H128 Acr B-	2	8	1
E. coli 7623 TolC-	8	128	16
K. pneumonia 1161486a TolC-	8	>128	32
P. aeruginosa PAO322	64	>128	32
A. baumannii BM4652 (efflux mutant)	NT	>128	32
cytotox IC_{50} (μg/mL)	NT	16	>36

[a]Compound described in ref 8. [b]Engineered bacterial strains lacking key efflux transporter proteins (e.g., AcrB, TolC).

Further analysis of the binding mode led us to the hypothesis that compound **12** almost certainly binds in an unfavorable conformation.[22] This is due to both steric (hydrogens) and electrostatic (heterocyclic nitrogen lone pairs) clashes between the pyridine and azaindazole rings (Figure 4). This is not the case in the more favored (unbound) conformation. Replacing the pyridine with a pyrimidine would remove the steric hindrance in the bound conformation and also create a clash (between nitrogen lone pairs) in the unbound conformation. Overall, this would contribute to stabilization of the bound state and therefore, hopefully, an increase in potency. Consequently, pyrimidine **13** [K_d (ITC) = 0.025 μM, LE = 0.45] (Figure 2) was prepared, which proved to be 15-fold more potent (compared to **12**).

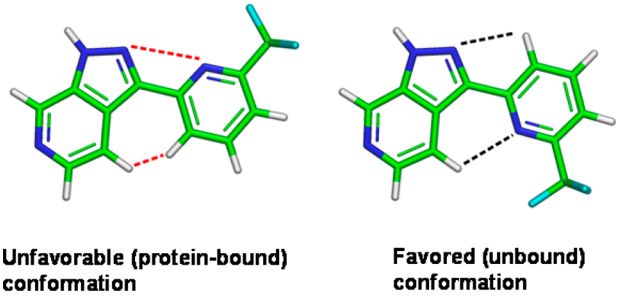

Figure 4. Illustration showing the alternative conformations of **12** (ethanolamine side chain removed for clarity).[22] Electrostatic and steric clashes are shown in red, and positive interactions are shown in black.

dx.doi.org/10.1021/ml4003277 | *ACS Med. Chem. Lett.* 2013, 4, 1208−1212

Compound **13** exhibited antibacterial activities (Table 1), with MIC values of 8 μg/mL or less against wild-type Gram-positive pathogens *S. aureus*, *S. pneumoniae*, and *S. pyogenes*. Moderate activities (16−32 μg/mL) were also seen against efflux mutants of Gram-negative pathogens such as *E. coli*, *P. aeruginosa*, and *A. baumannii*. The lack of activity against most wild-type Gram-negative strains suggested that compound **13** was subject to active efflux out of the cell. This may also be compounded with inadequate cell permeability. General cytotoxicity against a mouse lung lymphoma cell line was not observed for compound **13** up to the highest concentration tested (100 μM). MIC data for literature compound **1** is shown for comparison.[8]

Antibacterial activity was determined to be caused by inhibition of LigA using a strain of *S. aureus* engineered to overexpress DNA ligase (Table 2). MICs of compound **13** were found to correlate with expression levels of DNA ligase.

Table 2. MIC for 13 in *S. aureus* Parent and LigA Overexpression Strains[a]

	MIC (μg/mL) vs *S. aureus* RN4220			
	pYH4		pYH4-YerG (DNA ligase)	
compd	−	+	−	+
13	8	8	32/16	128

[a]pYH4 = vector control. pYH4-YerG = vector + DNA gene. +/− = with or without inducer (0.1 μg/mL anhydrotetracycline).

This result is consistent with a DNA-ligase mediated mode of antibacterial action in this species. In the Gram-negative pathogen *E. coli*, the mode of action was also tracked to LigA inhibition by showing cross-resistance with LigA target mutants (Table 3).[23]

Table 3. MIC for 13 in *E. coli* Efflux Mutant Parent and LigA Target Mutant Strains

	MIC (μg/mL)
E. coli	compd **13**
TOP10 Δ*Tol*C	8
TOP10 Δ*Tol*C LigA G180E	128/64
TOP10 Δ*Tol*C LigA R150S	128/64
TOP10 Δ*Tol*C LigA R518H	64
E. coli LigA IC_{50} (uM)	0.097

In summary, we have identified **13** (K_d = 25 nM, LE = 0.45, LLE_{AT} = 0.45[24]) as an inhibitor of bacterial DNA ligase. Starting from pyrazine fragment **3** (K_d = 38 μM, LE = 0.50, LLE_{AT} = 0.56), X-ray crystallographic data was used to establish key determinants for affinity and to guide structure based design. In particular, a strategy of establishing additional hydrogen bonds to the protein backbone and stabilizing the enzyme-bound conformation led to over a 1000-fold increase in activity, relative to starting point **3**. Good LE and lipophilic ligand efficiency (LLE_{AT}) were maintained during this process. Compound **13** demonstrated single-digit MICs across a range of Gram-positive pathogens, which, in the case of *S. aureus*, was shown to be target mediated. The 6-azaindaole scaffold provides a novel, nonpurine, chemotype to the LigA field, and to our knowledge, **13** is the first published example of a fragment-derived LigA inhibitor. Moreover, this work provides further validation of FBDD as an effective, complementary approach in the field of antibacterials.

■ ASSOCIATED CONTENT

Supporting Information

Assay conditions (including error limits and data for reference compounds), microbiology methods, biophysical methods, and synthetic procedure/characterization of compounds **4**−**13**. This material is available free of charge via the Internet at http://pubs.acs.org.

■ AUTHOR INFORMATION

Corresponding Authors

*(S.H.) Tel: 44-1223-226209. Fax: 44-1223-226201. E-mail: Steven.Howard@astx.com.

*(H.C.) Tel: 1-610-917-6983. E-mail: haifeng.2.cui@gsk.com.

Notes

The authors declare no competing financial interest.

■ ACKNOWLEDGMENTS

We would like to thank David Rees, Andrew Leach, and Richard Jarvest for useful comments on the manuscript; and Joe Coyle, Finn Holding, Alex Thomas, Sharna Rich, Alan Rendina, Miriam Burman, and Emma Jones for biophysics and assay support. Also, thanks to Nicola Wallis, Christopher Johnson, Glyn Williams, Jeff Yon, and Christopher Murray for providing their support during the project.

■ REFERENCES

(1) Shuman, S. J. DNA ligases: Progress and prospects. *J. Biol. Chem.* **2009**, *284*, 17365.

(2) Lehman, I. R. DNA ligase: Structure, mechanism and function. *Science* **1974**, *186*, 790.

(3) Tomkinson, A. E.; Vijayakumar, S.; Pascal, J. M.; Ellenberger, T. DNA ligase: Structure, reaction mechanism and function. *Chem. Rev.* **2006**, *106*, 687.

(4) Streker, K.; Schäfer, T.; Freiberg, C.; Brötz-Oesterhelt, H.; Hacker, J.; Labischinski, H.; Ohlsen, K. In vitro and in vivo validation of *ligA* and *tarI* as essential targets in *Staphylococcus aureus*. *Antimicrob. Agents Chemother.* **2008**, *52*, 4470−4474.

(5) Lavesa-Curto, M.; Sayer, H.; Bullard, D.; MacDonald, A.; Wilkinson, A.; Smith, A.; Bowater, L.; Hemmings, A.; Bowater, R. P. Characterisation of a temperature-sensitive DNA ligase from *Escherichia coli*. *Microbiology* **2004**, *150*, 4171−4180.

(6) Swift, R. V.; Amaro, R. M. Discovery and design of DNA and RNA ligase inhibitors in infectious microorganisms. *Expert Opin. Drug Discovry* **2009**, *4*, 1281−1294.

(7) Boucher, H. W.; Talbot, G. H.; Bradley, J. S.; Edwards, J. E.; Gilbert, D.; Rice, L. B.; Scheld, M.; Spellberg, B.; Bartlett, J. Bad bugs, no drugs: No ESKAPE! An update from the Infectious Diseases Society of America. *Clin. Infect. Dis.* **2009**, *48*, 1.

(8) Mills, S. D.; Eakin, A. E.; Buurman, E. T.; Newman, J. V.; Gao, N.; Huynh, H.; Johnson, K. D.; Lahiri, S.; Shapiro, A. B.; Walkup, G. K.; Yang, W.; Stokes, S. S. Novel bacterial NAD^+-dependent DNA ligase inhibitors with broad-spectrum activity and antibacterial efficacy in vivo. *Antimicrob. Agents Chemother.* **2011**, *1088*, 55.

(9) Stokes, S. S.; Huynh, H.; Gowravaram, M.; Albert, R.; Cavero-Tomas, M.; Chen, B.; Harang, J.; Loch, J. T., III; Lu, M.; Mullen, G. B.; Zhao, S.; Liu, C. F.; Mills, S. D. Discovery of bacterial NAD^+-dependent DNA ligase inhibitors: optimization of antibacterial activity. *Bioorg. Med. Chem. Lett.* **2011**, *21*, 4556.

(10) Surivet, J.-P.; Lange, R.; Hubschwerlen, C.; Keck, W.; Specklin, J.-L.; Ritz, D.; Bur, D.; Locher, H.; Seiler, P.; Strasser, D. S.; Prade, L.; Kohl, C.; Schmitt, C.; Chapoux, G.; Ilhan, E.; Ekambaram, N.; Athanasiou, A.; Knezevic, A.; Sabato, D.; Chambovey, A.; Gaertner, M.; Enderlin, M.; Boehme, M.; Sippel, V.; Wyss, P. Structure-guided

design, synthesis and biological evaluation of novel DNA ligase inhibitors with in vitro and in vivo anti-staphylococcal activity. *Bioorg. Med. Chem. Lett.* **2012**, *22*, 6705−6711.
(11) Wang, T.; Duncan, L.; Gu, W.; O'Dowd, H.; Wei, Y.; Perola, E.; Parsons, J.; Gross, C. H.; Moody, C. S.; Arends, R. S. J.; Charifson, P. S. Design, synthesis and biological evaluation of potent NAD^+-dependent DNA ligase inhibitors as potential antibacterial agents. Part II: 4-amino-pyrido[2,3-d]pyrimidin-5(8H)-ones. *Bioorg. Med. Chem. Lett.* **2012**, *22*, 3699−3703.
(12) Payne, D. J.; Gwynn, M. N.; Holmes, D. J.; Pompliano, D. L. Drugs for bad bugs: confronting the challenges of antibacterial discovery. *Nat. Rev. Drug Discovery* **2007**, *6* (1), 29−40.
(13) Murray, C. W.; Rees, D. C. The rise of fragment-based drug discovery. *Nat. Chem.* **2009**, *1*, 187−192.
(14) Eakin, A. E.; Green, O.; Hales, N.; Walkup, G. K.; Bist, S.; Singh, A.; Mullen, G.; Bryant, J.; Embrey, K.; Gao, N.; Breeze, A.; Timms, D.; Andrews, B.; Uria-Nickelsen, M.; Demeritt, J.; Loch, J. T., III; Hull, K.; Blodgett, A.; Illingworth, R. N.; Prince, B.; Boriack-Sjodin, P. A.; Hauck, S.; MacPherson, L. J.; Ni, H.; Sherer, B. Pyrrolamide DNA gyrase inhibitors: Fragment-based NMR screening to antibacterial agents. *Antimicrob. Agents Chemother.* **2012**, *56* (3), 1240−1246.
(15) Hudson, S. A.; McLean, K. J.; Surade, S.; Yang, Y. Q.; Leys, D.; Ciulli, A.; Munro, A. W.; Abell, C. Application of fragment screening and merging to the discovery of inhibitors of the *mycobacterium tuberculosis* cytochrome P450 CYP121. *Angew. Chem., Int. Ed.* **2012**, *51*, 9311−9316.
(16) Murray, C. W.; Verdonk, M. L.; Rees, D. C. Experiences of fragment-based drug discovery. *Trends Pharmacol. Sci.* **2012**, *33* (5), 224−232.
(17) O'Shea, R.; Moser, H. E. Physicochemical properties of antibacterial compounds: implications for drug discovery. *J. Med. Chem.* **2008**, *51*, 2871−2878.
(18) Manchester, J. I.; Buurman, E. T.; Bisacchi, G. S.; McLaughlin, R. E. Molecular determinants of AcrB-mediated bacterial efflux implications for drug discovery. *J. Med. Chem.* **2012**, *55*, 2532−2537.
(19) $LE = -\Delta G/HAC \approx -RT \ln(IC_{50})/HAC$. Hopkins, A. L.; Groom, C. R.; Alex, A. Ligand efficiency: a useful metric for lead selection. *Drug Discovery Today* **2004**, *9*, 430−431.
(20) Han, S.; Chang, J. S.; Griffor, M. Structure of the adenylation domain of NAD^+-dependent DNA ligase from *Staphylococcus aureus*. *Acta Crystallogr.* **2009**, *F65*, 1078−1082.
(21) Aqueous solubility measured by a HPLC method using ChemiLuminescent Nitrogen Detection quantification.
(22) Molecular calculations and NMR data to support this, together with precedence from the CCD, are described in the Supporting Information.
(23) Target mutants were generated using compound **1** (see Supporting Information).
(24) Mortenson, P. N.; Murray, C. W. *J. Comput. Aided Mol. Des.* **2011**, *25*, 663−667.